Acoustics 2002 - Innovation in Acoustics and Vibration
Annual Conference of the Australian Acoustical Society
13-15 November 2002, Adelaide, Australia

UNDERWATER EXHAUST NOISE

Christopher Norwood and Li Chen

Maritime Platforms Division, DSTO Melbourne
Australia, Victoria, 3030.
chris.norwood@dsto.defence.gov.au

1 INTRODUCTION

Conventional diesel-electric submarines require periodically to recharge the batteries, by running the diesel engines, commonly called snorting. The diesel exhaust can either be discharged into the atmosphere using a snort exhaust mast, or discharged underwater, through a fin top exhaust. There are advantages and disadvantages for each of the two methods.

The Collins class submarine uses an underwater exhaust, discharged through a fin top diffuser. This has been identified as an important noise source in the mid and high frequency regions. Flow noise was considered to be a likely contributor to the noise, as the design of the fin top exhaust had a number of undesirable flow features.

For a low Mach number flow, the dominant noise source factors are the fluctuations of wall pressure or drag force on the wall, You et al[1]. The generation of sound in a pipe system can be mainly attributed to the vibration of the pipe wall caused by the turbulent flow, throttling flow and bends. The sound will propagate along the pipe and through the fluid with the constriction of the flow and be radiated to the environment through the fluid exits and the pipe walls.

The fluctuation of wall pressure generated by turbulent internal pipe flow is proportional to the wall shear and a relationship between the corresponding sound power and the fluctuation of the wall shear can be derived, Blake[2]. Nelson and Morfey[3] assumed that the fluctuation of wall shear is proportional to the steady head loss in a pipe. This means that part of the work done by the head loss is dissipated by sound. For a low Mach number turbulent flow over a rigid surface Mak and Oldham[4] concluded that part of the total kinetic energy generated on surfaces is transferred into acoustic energy.

From these relationships it is assumed the sound power can be related to the steady-state total head loss in the system or the total turbulent kinetic energy on the surfaces. This would suggest that minimising these two quantities is an effective way to control the noise generation. For a pipe system, turbulence is mainly generated due to the walls, obstructions and bends. Therefore proper design of a pipe system, where turbulence is minimised, is crucial to the minimisation of the acoustic signature.

In this study, alternate fin top exhaust designs were analysed using CFD to determine the head loss and total kinetic energy. An improved design, which minimised these two parameters, was developed. Experimental measurements of the radiated noise from four different fin top

designs were made to compare the differences in head load and total kinetic energy to the differences in the radiated noise. The four designs were the original submarine exhaust, a DSTO improved design and two alternate designs proposed by Kockums AB, denoted 471-F and 471A12.

Despite large variations in the head loss and total turbulent kinetic energy for the four designs the experimental measurements on the four models showed little variation in the total radiated noise. Additional near field acoustic holography measurements on three of the models identified structural radiation and gas exit noise as the main noise sources. The bubble cloud noise and surface splash were not important noise sources.

2 CFD ANALYSIS

The flow in the exhaust system, which is highly turbulent, has a typical Reynolds number of $5x10^5$ based on the inlet pipe radius. The temperature change of the fluid was ignored. It was reasonable to assume that the exhaust gas was incompressible and isothermal. Due to its simplicity the k-ε type two-equation turbulent model, with a wall function, has been widely used in many engineering applications. In this study the RNG k-ε model of Yanhot et al[5] was adopted. In this case k is the turbulent kinetic energy (per unit mass) and ε is turbulent dissipation.

The commercial CFD package Fluent was used for the calculations. The SIMPLE algorithm was used for the velocity-pressure coupling, and the partial differential equations are discretised on a hybrid unstructured grid. More than 500,000 mesh points were used in the simulations.

The fin top exhaust outlets analysed are shown in Figure 1. The results of the CFD study for the current design and the two alternative designs are summarised in Table 1. Detailed analysis of the results showed that both the DSTO and 471-F designs resulted in more uniform velocity distribution through the outlet nozzles, with a consequent reduction in the peak velocities. The 471-F and 471A12 designs had a 30% reduction in total head loss, but the total turbulent kinetic energy was only reduced by 7%. The DSTO design showed a 79% reduction in total head loss and a 35% reduction in total turbulent kinetic energy.

3 MODEL TESTS CONDUCTED

Experimental measurements of the radiated noise from the original fin top design and the three alternate designs were made using one-quarter-scale exhaust models. The radiated noise from the models was measured using several hydrophones positioned in the “far field”. The radiated noise was measured for flow rates corresponding to full load flow and idle load flow in the real submarine.

A second phase of measurements, involving detailed scans of the radiated noise from the three alternate designs, using sound intensity and near field acoustic holography techniques was made. In these tests scans of the radiated noise on the forward side of the exhaust were made for all three models. Measurements were also made on the reverse side of the 471-F and

DSTO models. The measurements were made for two different flow velocities equivalent to idle flow and full load flow speeds in the full sized submarine exhaust.

The detailed scan measurements were made to attempt to identify the major noise sources from the fin top exhausts. Forward and reverse measurements allowed the presence of any screening from the bubble cloud to be identified. In addition, for one of the models, measurements were made with the exhaust wrapped in plastic bubble wrap, thus reducing structural radiation as a source. This allowed the relative importance of the structural radiation as a source to be determined. The measurements were made by scanning over a vertical plane 0.5m in front of the exhaust outlet, using an array of intensity probes. Both sound intensity processing and acoustic holography processing were used to determine the source levels for the different designs. Examination of both the holographic images and the sound intensity patterns was used to identify the main sources of the acoustic radiation for the model exhausts.

4 EXPERIMENTAL SET-UP

A schematic of the test arrangement is shown in Figure 2. The exhaust outlet was mounted in a frame that was lowered into the water so that the outlet was approximately 3m below the surface. The radiated sound pressure levels for the four models were measured by a series of "far field" hydrophones, which were placed at different distances in front of the exhaust outlet. The radiated noise was measured for two flow rates, which corresponded to full load and idle condition in the full size submarine exhaust.

For the second set of tests the sound field in a plane 0.5m from the exhaust outlet was scanned using a line of 21 sound intensity probes, Figure 3. The sound intensity probes were mounted on a horizontal beam, which in turn was mounted on two vertical columns. A simple cable and pulley mechanism was used to move the probes vertically. Measurement positions were marked on the vertical columns and the position of the horizontal bar was monitored using a pair of underwater video cameras. Figure 4 shows a model exhaust being lowered into the water on the measurement frame.

The sound intensity probes were mounted on the horizontal bar, at a spacing of 0.075m, giving an array length of 1.5m. The intensity probes consisted of pairs of Reson TC4013 hydrophones, arranged in a side-by-side configuration, with the distance between the hydrophones being 0.025m. This gave an upper frequency limit for the intensity probe of 10000 Hz. The hydrophones were individually calibrated using a Bruel and Kjaer piston phone with a hydrophone adapter. The phase matching between the hydrophone pairs was measured using an intensity probe calibrator mounted on the Bruel and Kjaer microphone calibrator, fitted with an adaptor for hydrophones. The phase matching was checked at 250 Hz and 1000 Hz using narrow band sources, and up to 5000 Hz using a broadband source. The hydrophone pairs were phase matched to better than 0.5^{o}.

Measurements were made over the scan plane at 0.075m vertical spacing, with the lowest position approximately 0.75m below the orifice of the exhaust outlet. This spacing gave a maximum frequency for the nearfield acoustic holography processing of 10000 Hz. The minimum dimension of the scan plane governs the lower frequency limit for the measurements. In this case the minimum dimension was 1.5m, giving an effective lower

frequency of 1000 Hz. However, unlike the upper frequency limit, the lower frequency limit is not a sharp cut off; but rather indicates the frequency below which the results become less reliable.

The data acquisition system consisted of a VXI chassis with four, 16-channel HP 1432A A/D cards, with a sample rate of 51.2 kHz. The chassis was fitted with an HP E8491A controller card, connected to a PC by a “firewire”. The data were stored on the computer hard disc, in addition all data were recorded on a 64-channel Sony SIR 1000 digital tape recorder. The data for every second probe were analysed in real time using a 24-channel HP 3566A analyser, configured as a 12 pair intensity analyser. The cross spectra for these intensity probes was analysed at an 8 Hz spacing as a check on the results from the holography processing system.

Bruel and Kjaer four channel Nexus charge amplifiers were used to provide signal conditioning for the hydrophones. In addition to the intensity probes six references were used. Three were placed in fixed locations on the measurement frame, and three were placed approximately 4, 6 and 10m from the frame. These references were used for the acoustic holography processing.

Measurements were made at either 46 or 24 vertical locations, which gave vertical measurement spans of 3.375 m and 1.725m respectively. The closest distance between the measurement probes and the exhaust outlet was 0.5m.

Measuring the stagnation pressure and static pressure at a point upstream of the model monitored the airflow velocity in the model. Measurements were made at two standard flow velocities corresponding to the idle and full flow velocities in the full sized submarine exhaust.

5 EXPERIMENTAL RESULTS

The radiated sound pressure levels for the four outlets in one-third octave bands from 1000Hz to 8000Hz are shown in Figure 5 for the two different flow rates. For the full flow condition the original exhaust shows two strong peaks in the radiated noise in the 2500 and 5000 Hz bands. The levels for the three modified exhaust systems are generally similar and lower than the original. Overall the 471A12 appears to be marginally quieter than the other two designs. The idle flow results appear less reliable. The radiated noise from the original is lower than for the three modified designs, and all four exhausts have the same levels from 5000 Hz to 8000 Hz. The difference in the radiated noise levels for the two flow rates varies across the frequency range. For the 1000Hz one-third octave band the levels for idle are approximately 4dB lower than the full flow levels. This difference reduces as the frequency increases and for the 8000 Hz one-third octave band the difference is approximately 1 dB.

Plots of the pressure at the measurement plane and the back projected pressure in the plane of the orifices over two wide bands, 1000 Hz to 5000 Hz and 5000 Hz to 10000 Hz, are shown in Figures 6 and 7 for the 46 position measurement scan, up to the surface, for model 471-F. These plots clearly show that the pressure levels in the upper bubble cloud and near the surface are much lower than the levels at the exhaust pipe or in the bubble cloud at the exhaust outlet. It can therefore be concluded that the radiated noise from the bubble cloud and the surface splash is much lower than for the gas exit and the structural radiation.

ISBN 0-909882-19-3

The radiated noise back projected to the plane of the orifices over the two wide frequency bands, is shown for the three exhaust outlet models tested. The plots show that structural radiation from the exhaust is the strongest source for each of the models. For the 471-F and 471A12 models both the vertical and horizontal pipe sections are strong radiators, while for the DSTO model the vertical pipe is a strong radiator, but there is little structural radiation from the horizontal pipe. The high levels in the vertical pipe for the DSTO model appear to be generated in the curved transition between the vertical and horizontal pipes.

The radiated noise levels for the reverse measurements, made on the 471-F and DSTO models were higher than the corresponding forward facing measurements, indicating the presence of some screening of the structural radiation by the lower part of the bubble cloud. The differences for the 471-F were higher than for the DSTO model, indicating a higher level of screening. Back projection of the radiated noise scans to the model exhaust for the reverse measurements showed that for the 471-F model the highest structural radiation occurred in the horizontal section of the model. While for the DSTO model the highest levels of structural radiation occurred in the curved transition between the vertical and horizontal sections. The peak levels for the DSTO model are higher than the 471-F model, but the radiating area appears lower.

These results are consistent with the results of the CFD analysis, which showed the DSTO model had smoother and less turbulent flow in the horizontal pipe section. What is not immediately apparent is why the DSTO model had such high structural radiation from the curved transition section. This could be due to localised flow separation in the curved pipe section.

6 CONCLUSIONS

Experimental measurements have shown that the main noise sources for the fin top exhaust are structural radiation and gas exit noise from the orifices. By redesigning the fin top exhaust outlet, considerable reductions in the head loss and total turbulent kinetic energy in the gas flow can be achieved. This should in turn lead to reductions in the radiated noise from the fin top exhaust. Experimental measurements of different designs have shown that the potential noise reductions did not occur and investigations into the reasons for this insensitivity are the subject of one going work.

.

7 REFERENCES

1. D.Y. You, H. Choi, M.R. Choi and S.H. Kang, 1998, *Control of flow-induced noise behind a circular cylinder using splitter plates*, AIAA Journal, **Vol** 36(11), pp1961-1967
2. W. Blake, *Mechanics of flow-induced sound and vibration*, Academic Press Inc.
3. P.A. Nelson and C.L. Morfey, 1981, *Aerodynamic sound production in low speed flow ducts, J Sound and Vibration*, **Vol** 78(2), pp 263-286
4. C.M Mak and D.J Oldham, 1995, *The application of computational fluid dynamics to eh prediction of regeneration noise in ventilation systems*, Inter-Noise, Newport Beach CA, July 10-12, pp 281-284

8 ACKNOWLEDGEMENTS

The authors wish to acknowledge the assistance of Kockums AB in the conduct of the experimental tests.

CASE	TTKE	THL
Original Exhaust	54.94	310.63
471-F	51	201.71
DSTO design	35.43	66.03
471A12	49.8	200.45

Table 1 Comparison of Total Turbulent Kinetic Energy (TTKE and Total Head Loss (THL) predictions for the four exhaust outlet designs

Figure 1. Exhaust outlet designs
(a) Existing submarine exhaust, (b) Alternate design 1,
(c) Alternate design 2 (DSTO), (d) Alternate design 3 (471A12).

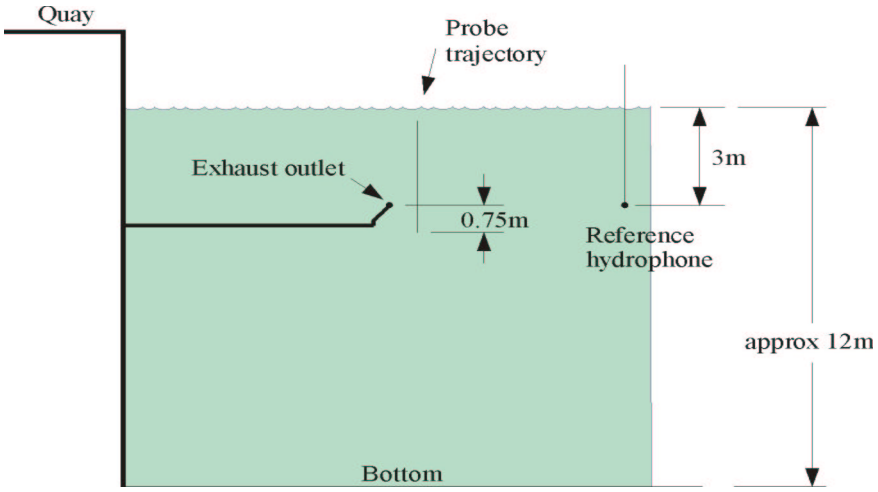

Figure 2 Schematic of test arrangement

Figure 3 Hydrophone probe array

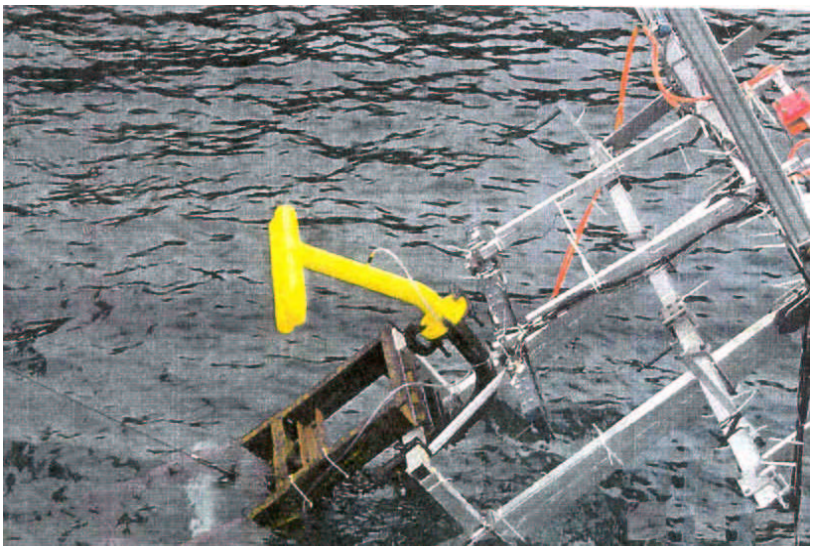

Figure 4 Test assembly being lowered into position for reverse measurement

ISBN 0-909882-19-3

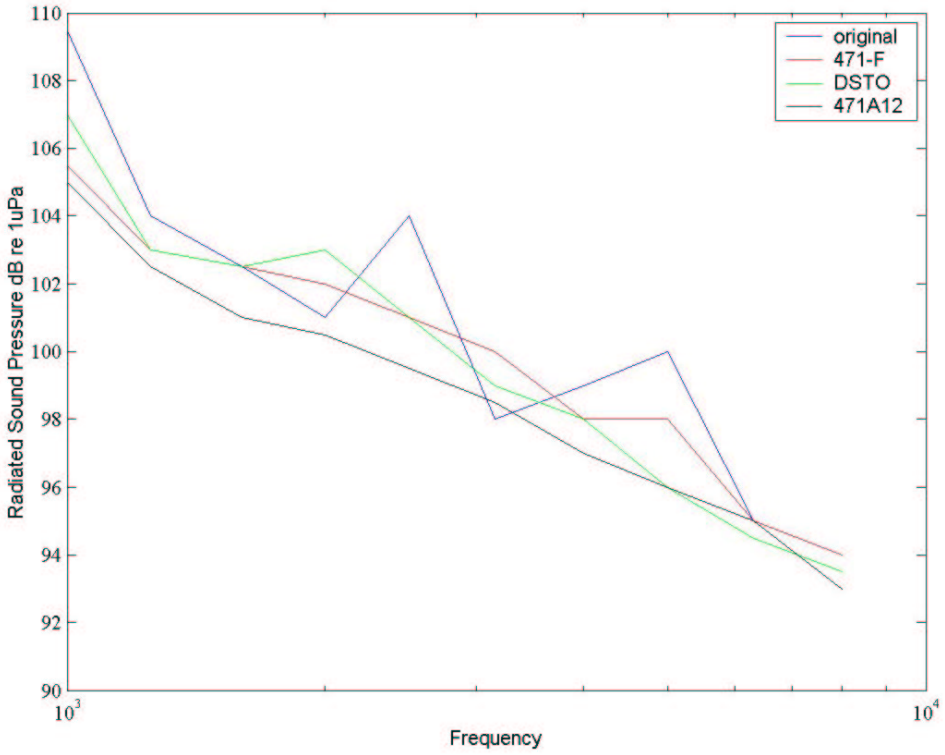

(a) Full Flow

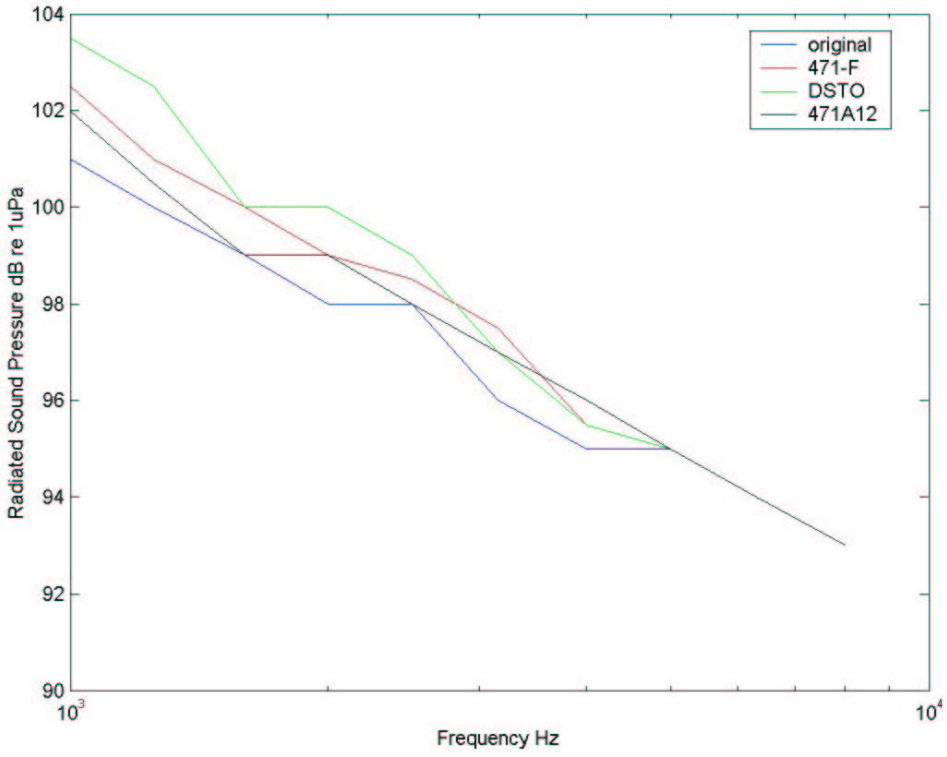

(b) Idle Flow

Figure 5 “Far Field” Radiated Sound Pressure

ISBN 0-909882-19-3

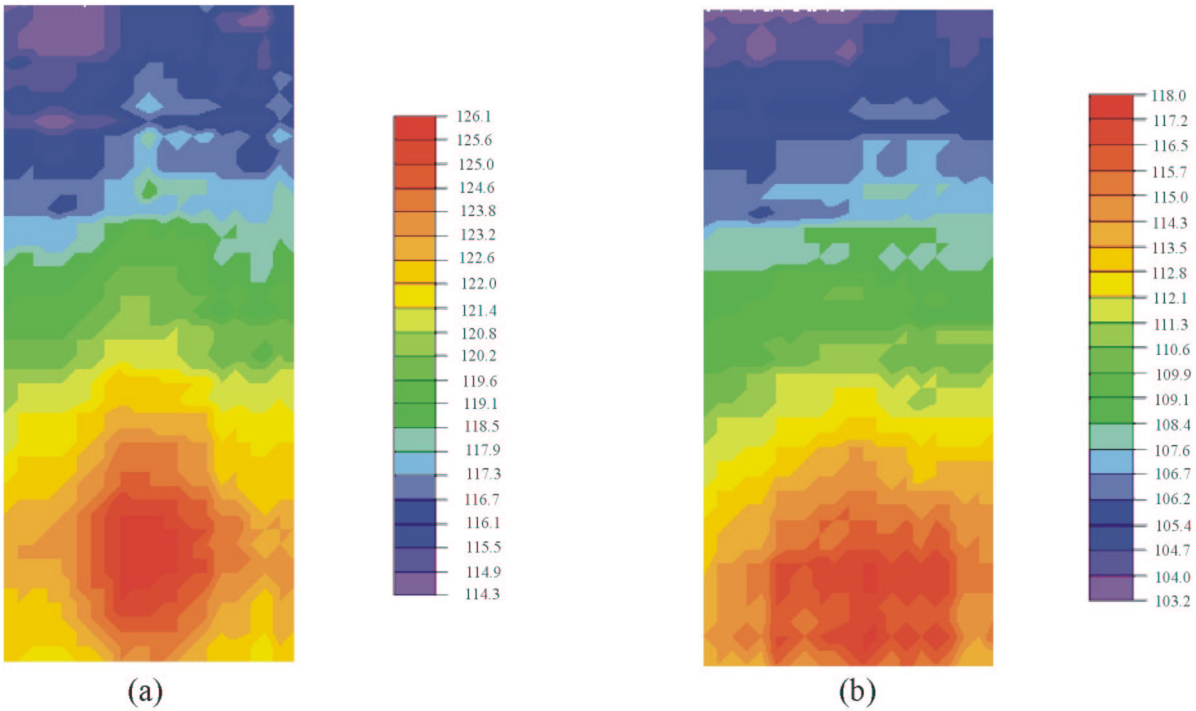

Figure 6 Pressure level at the measurement plane
(a) 1000-5000Hz (b) 5000-10000Hz

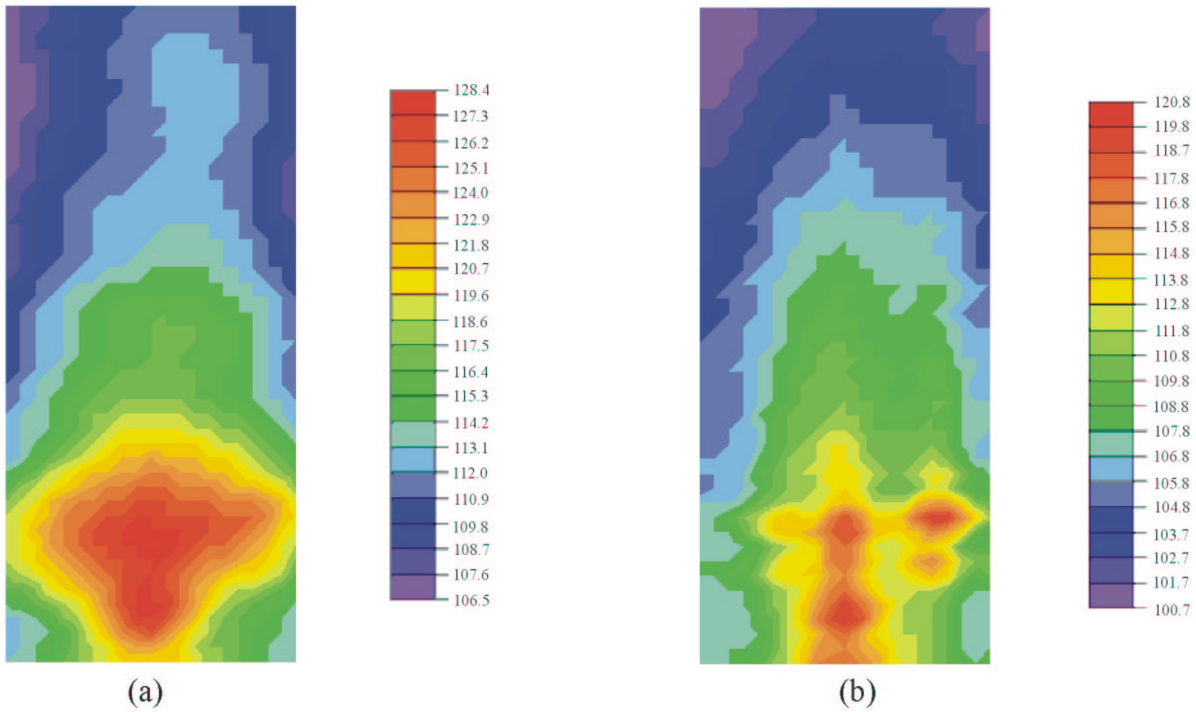

Figure 7 Pressure level at the plane of the orifice.
(a) 1000-5000Hz (b) 5000-10000Hz

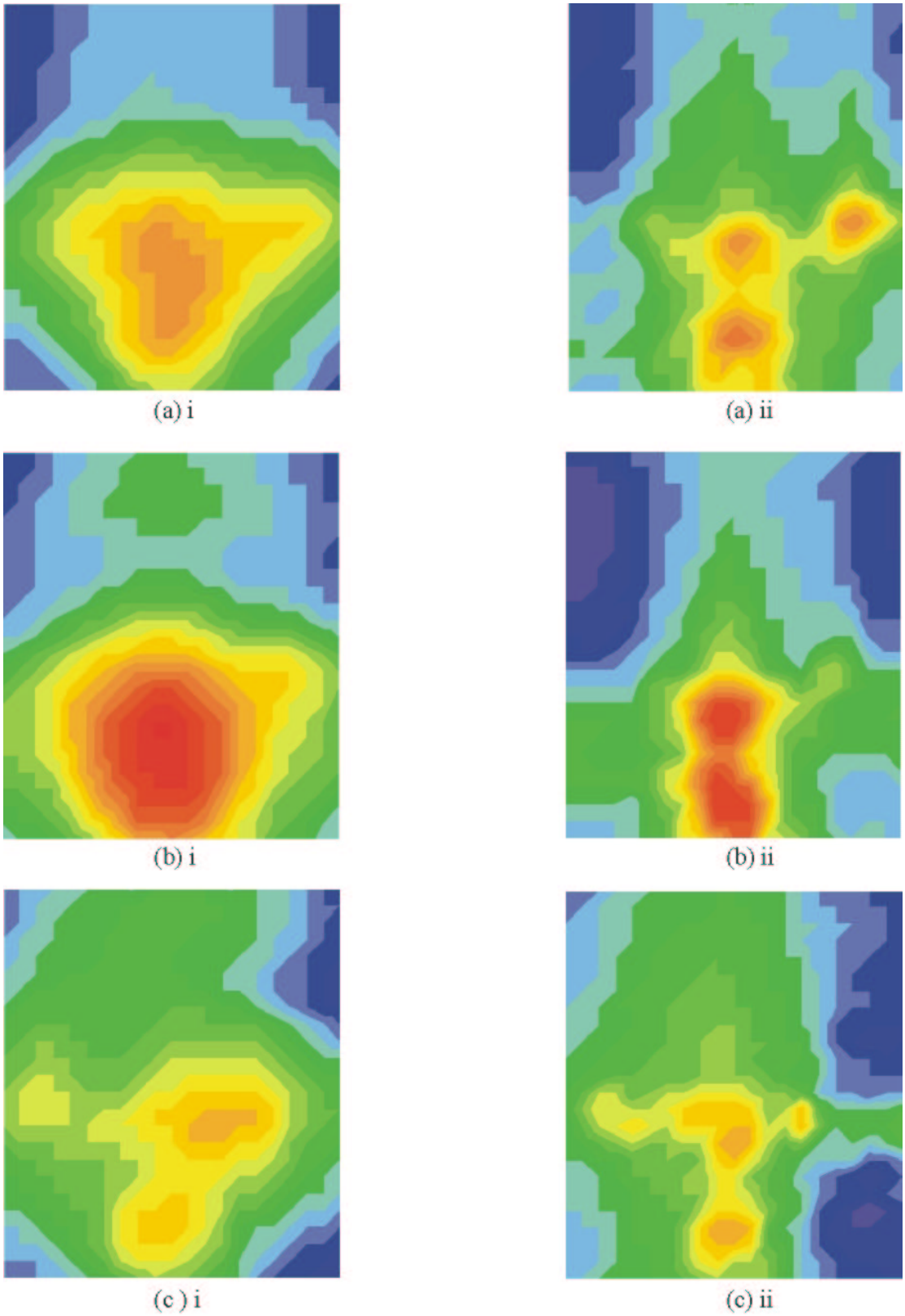

(a) i (a) ii

(b) i (b) ii

(c) i (c) ii

Figure 8. Pressure level back projected to the plane of the orifice
(a) Model 471-F , 1000-5000 Hz. i, 5000- 1000 Hz ii.
(b) DSTO Design , 1000-5000 Hz i, 5000-10000 Hz ii.
(c) Model 471A12 , 1000-5000 Hz i, 5000-10000 Hz ii.